Applied Surface Science 589 (2022) 152971

Contents lists available at ScienceDirect

Applied Surface Science

journal homepage: www.elsevier.com/locate/apsusc

Full Length Article

2D-Mo_3S_4 phase as promising contact for MoS_2

E.V. Sukhanova [a,*], A.G. Kvashnin [b], L.A. Bereznikova [a,c], H.A. Zakaryan [d], M.A. Aghamalyan [d], D.G. Kvashnin [a,c], Z.I. Popov [a,*]

[a] Emanuel Institute of Biochemical Physics RAS, 119334, 4 Kosigin st., Moscow, Russia
[b] Skolkovo Institute of Science and Technology, Skolkovo Innovation Center 121205, Bolshoy Boulevard 30, bld. 1, Moscow, Russia
[c] Moscow Institute of Physics and Technology (National Research University), 9 Institutskiy per., Dolgoprudny, Moscow Region 141701, Russia
[d] Yerevan State University, 1 Alex Manoogian st., Yerevan, Armenia

A B S T R A C T

The search for electrode materials for two-dimensional structures, particularly for semiconducting H-MoS_2, is a significant problem for contemporary materials science. This stimulates interest in metastable structures, which motivates us to look at non-stoichiometric metastable states known as Berthollides. An unbiased evolutionary search for new two-dimensional structures in Mo-S system showed the presence of Mo_5S_4, Mo_3S_4, and MoS metastable structures (located near the decomposition line) in the low-sulfur area of phase diagram. The predicted novel *Cm*-Mo_3S_4 phase exhibits metallic properties and dynamic stability confirmed by the calculation of phonon dispersion spectra. Its lattice parameters are similar to the semiconducting H-MoS_2 phase which makes it possible to use *Cm*-Mo_3S_4 as a conducting contact in nanodevices based on MoS_2. A study of proposed H-MoS_2/*Cm*-Mo_3S_4 lateral heterostructures showed that in the contact region a transition to the conducting states of the H-MoS_2 edge atoms is observed, as well as the preservation of *Cm*-Mo_3S_4 conducting properties. The main feature of *Cm*-Mo_3S_4 is that it can be structurally obtained by a direct transition of H-MoS_2 monolayer with sulfur vacancies. As a result, the predicted *Cm*-Mo_3S_4 phase is a promising candidate for conducting contacts in nanoelectronic device components.

1. Introduction

The intensive development of two-dimensional field in material science starts in 2004 since graphene was synthesized for the first time [1]. Among recently synthesized 2D nanomaterials, particular emphasis should be placed to the family of transition metal dichalcogenides (TMD), namely molybdenum disulfide (MoS_2). Several 2D MoS_2 phases with exact 1:2 stoichiometry are known, and they exhibit a wide range of electronic characteristics, from semiconducting [2,3] and metallic [4] to ferromagnetic semimetallic [5] and topological insulating [6–13]. Among all 2D MoS_2 compounds, the energetically favorable and stable phase is a semiconducting H-MoS_2 [14] with hexagonal structure and *P6/mmc* space group symmetry. H-MoS_2 phase is widely studied and used in practical applications due to its unique physical and chemical features [15] that vary with thickness of material. Thermal stability [16], direct band gap and high charge carrier mobility [17], fluorescence in the visible range of light made MoS_2 a promising material for application in the scientific and technical fields [18] like energy harvesting and conversion [19–21], opto- and nanoelectronics [22,23], sensing [24], spintronics [25] and even in surface catalysis [26].

There are several reports about the application of H-MoS_2 as a key element in field-effect transistor, which is characterized by a huge ON/OFF current ratio and near-theoretical subthreshold swing values [27,28]. It should be noted that transistor characteristics are mainly determined by the quality of contact with metallic electrodes. The existence of the Schottky barrier at the interface with MoS_2 sample prevents electron transport [29–31]. To improve the properties of electronic circuits based on MoS_2, metallic electrodes with a low work function must be used [17,32], or MoS_2 layers must be doped [33–35]. Another method of lowering the Schottky barrier is using metallic T-phase of MoS_2 as electrodes [36–40] that can be covalently bonded with semiconducting H-phase, resulting in the formation of the lateral heterostructure.

Heterostructures generally consist of two or more different 2D materials chemically connected with each other to form a continuous monolayer. Current technology is ready to synthesize heterostructures of various compositions by edge epitaxy [41–43], while the heterostructures of various phases can usually be obtained via phase transition of the portion of the sample, for example, caused by ion beam irradiation [44,45] or intercalation by metal atoms [46]. It is possible to observe Ohmic contact in a multi-phase lateral structure, which significantly reduces the height of the charge transfer barrier [37]. The creation of Ohmic contacts via phase transition should imply that both phases must be stable (thermodynamically and dynamically). It was reported in

* Corresponding authors.
E-mail addresses: yekaterina.sukhanova@phystech.edu (E.V. Sukhanova), zipcool@bk.ru (Z.I. Popov).

https://doi.org/10.1016/j.apsusc.2022.152971
Received 22 November 2021; Received in revised form 18 February 2022; Accepted 28 February 2022
Available online 9 March 2022
0169-4332/

Ref. [47] that the metallic T-MoS_2 phase can be produced through structural changes that occur during Li intercalation. However, annealing at moderate temperatures (~200 °C) forces reverse transformation to the initial H-MoS_2 phase [47]. This fact significantly limits a longstanding application of such contacts and thus the challenge of identifying novel techniques to form contacts with MoS_2 is important and must be resolved. One solution to this problem is to stabilize metallic phases by breaking the stoichiometry of MoS_2, which will prevent the transition to the semiconducting phase from occurring owing to the shortage of the components.

Two centuries ago, French chemist Claude Louis Berthollet defended the idea of indeterminate chemical compositions, which was far ahead of his time and has found wide application in modern low-dimensional materials chemistry [48,49]. Binary compounds which can form non-stoichiometric compositions are called Berthollides. Such compounds are formed when defects are introduced into a known stoichiometric stable structure, resulting in a change in stoichiometry [50]. Changing the stoichiometry is possible through ion beam irradiation [50] during which the lighter element (in our case chalcogen atom) will be partially removed from the TMD surface. In this regard, the search for new, conducting, and thermodynamically stable two-dimensional phases in the Mo-S system seems promising for the creation of lateral hetero-structured compounds with the H-MoS_2 phase.

Here we present the results of the evolutionary search for novel two-dimensional Mo-S phases with various stoichiometries. Among known structures, we found a novel Mo_3S_4 phase which demonstrates kinetic stability and exhibits metallic properties. *Ab initio* calculations were used for a comprehensive investigation of the physical and chemical properties of the Mo_3S_4 phase. Predicted novel Mo_3S_4 phase can find possible application as conductive contacts for H-MoS_2 samples in electronic and optoelectronic devices, as supported by electronic properties calculation of H-MoS_2/*Cm*-Mo_3S_4 lateral interfaces.

2. Computational details

The search for new 2D compounds in the Mo-S system was performed via a variable-composition evolutionary algorithm as realized in the USPEX package [51–53]. During the search, the thickness of the predicted two-dimensional materials was limited to the range of 0–6 Å, while the number of atoms in the unit cell was varied from 4 to 16. In the first generation, 180 structures were considered, each subsequent generation consisted of 120 new structures, 50% of which was obtained using heredity, 30% was obtained using a random symmetric structure generator [54], 10% of the structures were generated using the lattice mutations and 10% were generated using the softmutation or coormutation operator. Additionally, fixed-composition searches were conducted for certain stoichiometries that were determined to be stable during the variable-composition search.

Structure optimization was carried out using quantum mechanical calculations within the density functional theory (DFT) as realized in the VASP program package [55–57]. To calculate the exchange–correlation functional the generalized gradient approximation (GGA) was used in Perdew – Burke – Ernzerhof (PBE) parameterization [58]. Ion-electron interaction was described by the augmented plane waves method (PAW) [59] with the energy cut-off of plane waves being equal to 520 eV. The sampling of the first Brillouin zone into a grid of k-points was carried out with a k-space resolution of $0.02 \times 2\pi \cdot Å^{-1}$ in periodic directions within the Monkhorst-Pack scheme [60]. The relaxation of the atomic geometry was carried out until the maximum value of interatomic forces became less than 10^{-2} eV/Å. The distance between the periodically located images was set to be no less than 15 Å to avoid the artificial influence of the layers on each other in a non-periodic direction. The resulting structures were selected by thickness with the final limitation of $l \leq 3.5$ Å since the thickness of T'-MoS_2 monolayer was used as a reference, calculated as the distance along the z-axis between the two most distant sulfur atoms. To estimate the dynamic stability of

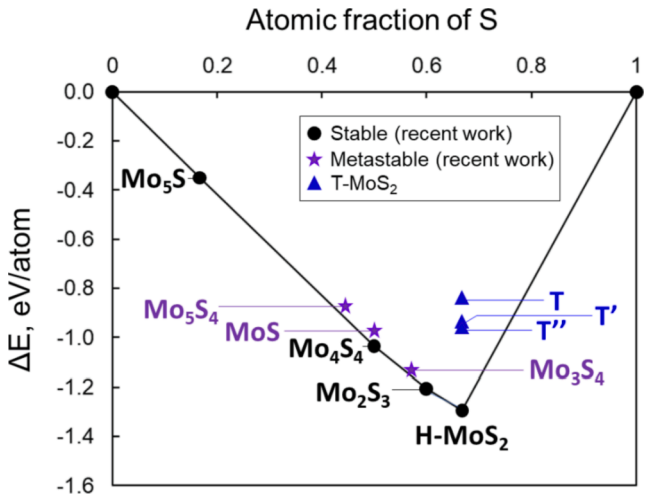

Fig. 1. Calculated convex hull of Mo-S system. Black, purple, and blue colors referred to predicted thermodynamically stable, novel metastable structures (≤0.1 eV/atom above convex hull), and known metastable T phases of MoS_2 respectively. (For interpretation of the references to color in this figure legend, the reader is referred to the web version of this article.)

obtained structures we calculated phonon dispersion spectra using the PHONOPY [61] software package. Transition states were determined using the climbing image nudged elastic band (CI-NEB) method [62,63]. VESTA [64] software was used for atomic structure visualization.

3. Results and discussion

An unbiased variable-composition search was used to predict a set of phases among possible Mo-S compounds. Calculated energy of formation – composition phase diagram is shown in Fig. 1, where predicted stable and metastable compounds together with already known phases (included T-MoS_2, T'-MoS_2, and T''-MoS_2 and studied earlier) are presented. Predicted thermodynamically stable (MoS_2, Mo_4S_4, Mo_5S, Mo_2S_3) phases are shown by black circles in Fig. 1. Independent fixed-composition searches were carried out for four stoichiometries corresponding to stable structures showing similar best structures to the ones we found in the variable-composition search. Detailed information about the atomic geometries of predicted structures is presented in Fig. S1 in Supplementary Information. Energies of formation of known metastable T-phases (T, T', T'') of MoS_2, which were theoretically investigated previously and some of them were successfully synthesized [65,66], are shown by blue trianlges. It should be noted, that T-phases of MoS_2 are located quite far from the calculated convex hull (more than 0.45 eV/atom) and the relative location of these phases correlates with Ref. [8]. Our calculations confirmed that the H-MoS_2 phase is thermodynamically stable, which is usually synthesized by the CVD technique as well as micromechanical exfoliation [67,68].

The most important property of newly predicted two-dimensional structures which defines the prospects of their application in technological fields is dynamic stability. For all predicted Mo-S compounds except for MoS_2, we calculated phonon band structures (see Fig. S2 in Supplementary Information). Since the structure and properties of MoS_2 phases are well studied [2,65,66] we did not pay attention to this issue in our work.

We found that among six predicted structures only four of them demonstrate the absence of imaginary phonon modes, which states the dynamical stability of considered structures. Minor imaginary modes near the Γ-point are associated with out-of-plane vibrational modes or caused by the lack of the rotational invariance consideration [69,70] (for more details see Supplementary Information section SI). In the left (Fig. 2 a,b) and right (Fig. 2 c,d) panels the atomic geometries and

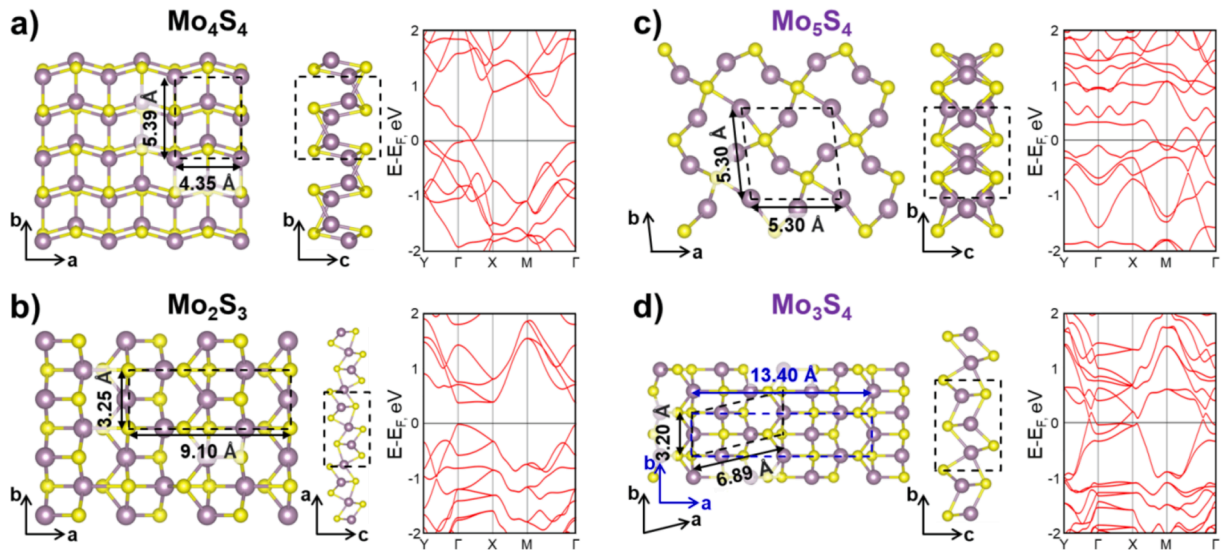

Fig. 2. The atomic structures and electronic band structures of predicted dynamically and thermodynamically (a, b) stable and (c, d) metastable Mo-S phases. Unit cells are indicated by black dotted lines. Purple and yellow colors correspond to Mo and S atoms respectively. (For interpretation of the references to color in this figure legend, the reader is referred to the web version of this article.)

calculated electronic band structures of dynamically stable and metastable structures are shown respectively. Orthorhombic structure of Mo_4S_4 (Fig. 2 a) was first predicted in Ref. [50] and for this phase, the areas of stability with respect to the chemical potential of sulfur were studied in Ref. [3]. Beyond the dynamic stability, the Mo_4S_4 structure displays a semimetallic band structure, which could be highly desirable for nanoscale device applications. Mo_2S_3 structure (Fig. 2 b) has a *Pmc*2_1 space group and exhibits semiconducting properties with a band gap of 0.4 eV which is consistent with previously reported results [3]. Both experimental and theoretical data indicate the stability of this structure [3]. An important feature of this phase is the coincidence of the *b* unit cell parameter with those of MoS_2. In this manner, the lateral heterostructure consisting of alternating of H-MoS_2 and Mo_2S_3 was theoretically studied [71]. The formation of 1D-electron gas with high mobility at a certain width of the H-MoS_2/Mo_2S_3 lateral heterostructure components was found in Ref. [71].

Special attention should be paid to metastable structures with energies of formation located close to the convex hull (not higher than 0.1 eV/atom) since these structures might be considered possibly attainable in fixed element ratios. Only three metastable phases (Mo_5S_4, Mo_3S_4, and MoS) satisfy the reduced criterion (purple stars in Fig. 1) and it should be noted that among considered two-dimensional metastable phases only MoS structure was studied previously [3]. Here we predicted two new dynamically stable phases with compositions of Mo_5S_4 (*Amm*2 space group) and Mo_3S_4 (*Cm* space group), see Fig. 2 c,d. Both metastable phases demonstrate metallic behavior according to the calculated electronic band structures.

The newly predicted Mo_3S_4 deserves special attention. It is interesting to note that Mo_2S_3 and Mo_3S_4 phases can be represented as alternation of structural elements of MoS (see Fig. S1 in Supplementary Information) having four-coordinated Mo atoms with regions of five-coordinated Mo atoms which stabilizes unstable MoS structure with changes of composition. Therefore, the Mo_3S_4 phase consists of 3 inequivalent molybdenum atoms, two of which are 5-coordinated and the third one is 4-coordinated. The 4-coordinated Mo atoms at tetrahedral surroundings of sulfur atoms correspond to the d-orbitals splitting to e_g below and the T_{2g} above. At the same time, 5-coordinated atoms have trigonal bipyramidal and square pyramidal geometry with correspondingly four and three *d*-orbitals below the initial energy level (see Fig. S6). We performed a Bader charge analysis [72] and found that Mo atoms have positive charges of 0.89 *e* in the square pyramidal surrounding, 0.83 *e* in the trigonal bipyramidal, and 0.72 *e* in the tetrahedral.

We additionally estimated the elastic properties of Mo_3S_4 phase. The 2D linear elastic constants calculated for Mo_3S_4 were determined to be $C_{11} = 129.6$ N/m, $C_{22} = 135.1$ N/m, and $C_{12} = 31.9$ N/m which indicate the near isotropic nature of the material. For considered orthorhombic unit cell calculated elastic constants satisfied Born elastic criteria [73] which states the elastic stability of the material (for more details see Supplementary Information section SII).

Another extremely important feature of the new phase is that it could be formed directly by applying mechanical deformations from the H-MoS_2 phase with the double S-vacancy line structure in the staggered configuration, which is the lowest energy configuration in many TMDs [74]. The formation of sulfur vacancies generally can be achieved by ion beam irradiation [50,75]. We also found that the total energy of *Cm*-Mo_3S_4 is lower than the energy of defective H-MoS_2 (H-Mo_3S_4) on 2.46 eV/f.u. and this fact means that the *Cm*-Mo_3S_4 is more thermodynamically stable than the defective H-phase. We performed DFT calculations of transition barrier from H-Mo_3S_4 to *Cm*-Mo_3S_4 phase by using CI-NEB [62,63] method with selective dynamics to fix Mo-sublattice at each step. It should be noted that the calculated barrier does not include the external pressure that must be applied for the phase transition. The resulting transition pathway and energy profile contain two maxima TS1 = 1.75 eV and TS2 = 0.95 eV that correspond to the structures of intermediate stages in Fig. S7, it is comparable with the barrier value for the transition from H-MoS_2 to T-MoS_2 (~1.5 eV) [76,77]. The local minimum between these two maxima is the structure IS = 0.55 eV. The obtained barriers can be overcome through exposure to the high temperature. In addition, the barrier from IS into the initial state (1.2 eV with respect to IS) is higher than the TS2 barrier (0.4 eV with respect to IS) and this indicates that the transition to the *Cm*-Mo_3S_4 phase is preferable.

Obtained results indicate the possibility of creating metallic regions within/or surrounded by semiconducting MoS_2. This is an incredibly promising method for fabricating lateral heterostructures composed of a central area (scattering region) and electrodes of identical composition that are linked uniformly (continuously) to the central region. Moreover, estimations of the lattice parameters of H-MoS_2 and *Cm*-Mo_3S_4 phases show the smallest lattice mismatch among all predicted phases, less than 1% in one direction (axis *b* in Fig. 2d, see Table S1 in Supplementary Information). This fact allows us to state with confidence the possibility of formation of heterogeneous lateral H-MoS_2/*Cm*-Mo_3S_4

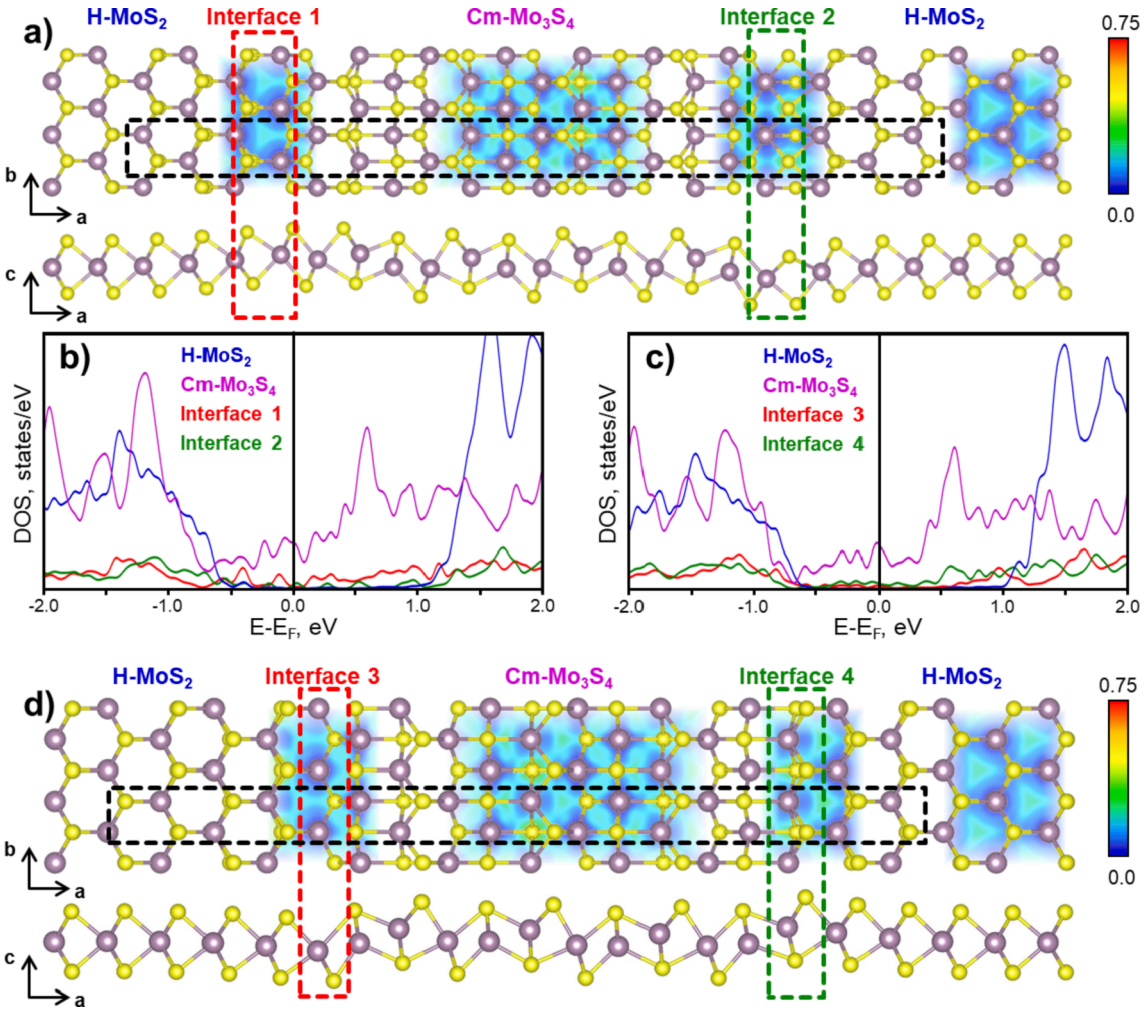

Fig. 3. Considered *Cm*-Mo_3S_4/H-MoS_2 lateral heterostructures: (a, d) the atomic structure. By purple and yellow colors Mo and S atoms are depicted. Color inserts: electron localization functions (ELF) for selected areas of lateral heterostructures. (b, c) Total and partial densities of electronic states (PDOS) for selected areas of considered *Cm*-Mo_3S_4/H-MoS_2 lateral heterostructures. The PDOSs are magnified by 4 times. The Fermi level E_F is set to zero. (For interpretation of the references to color in this figure legend, the reader is referred to the web version of this article.)

structure which could be represented as alternation of metallic and semiconducting regions within one layer of the same compositions.

To define the properties of contacts made of *Cm*-Mo_3S_4 (metallic regions) together with the semiconducting MoS_2 region within the heterostructure we simulate four possible interfaces between H-MoS_2 and *Cm*-Mo_3S_4 phases (labeled by red and green color in the Fig. 3a,d). Interfaces were distributed along the zigzag edge of H-MoS_2, have no atom excess or deficiency, are atomically smooth, and the lateral size of each region was selected to be more than 10 Å to avoid an influence of interfacial regions on the electronic structure of individual phases of the heterostructure. For simulations of heterostructure, the rectangular unit cell depicted by blue lines (Fig. 2d) was considered in the case of the Mo_3S_4 phase.

For each component of heterostructure (including interfacial regions and the atoms at the center of the H-MoS_2 and *Cm*-Mo_3S_4 nanoribbons) we also analyzed partial density of electronic states (PDOS) (see Fig. 3b, c). Our calculations prove that MoS_2 and Mo_3S_4 retain their electronic characteristics even become connected to heterostructure: MoS_2 retains semiconducting properties with the band gap of 1.7 eV, while Mo_3S_4 still exhibits metallic properties (blue and purple curves in Fig. 3b,c, respectively). One can see non-zero density of states at the Fermi energy (see Fig. 3b,c) like in the case of polycrystalline MoS_2 monolayers [78] which indicates the metallization of the boundary atoms. Moreover, the lack of sharp peaks at the Fermi energy demonstrates the covalent bonding at the interface area which additionally proved by the electron localization function (ELF) of interfacial regions. ELF gives a pattern of the transition of electrons from localized (H-MoS_2 region) to delocalized states (*Cm*-Mo_3S_4 region), see insets in Fig. 3a,d. The ELF color bar illustrates the rate of electron localization in each section of the investigated heterophase structures.

Band alignment is an important property of the interface. One of the most important characteristics of metal–semiconductor heterojunction is the Schottky barrier height defining the charge transfer through the interface. To estimate the Schottky barrier height of the *Cm*-Mo_3S_4/H-MoS_2 lateral heterostructures we used the Schottky-Mott model which neglects the metal–semiconductor interaction and therefore the model does not consider Fermi-level pinning. The contact properties depend on the ratio between the work function of the metal electrode (Mo_3S_4) and the electron affinity/ionization potential of the semiconductor (MoS_2). The calculated work function value of the pristine *Cm*-Mo_3S_4 metallic phase is 5.06 eV while the electron affinity and ionization potential of the MoS_2 phase are 4.18 eV and 5.90 eV, respectively, which are consistent with previously reported results [79–81] (for more details Section SIV in Supplementary Information). The resulting values of barrier heights are $\Phi_e^{SM} = 0.88$ eV and $\Phi_h^{SM} = 0.84$ eV for electrons and holes respectively (for more details Section SIV in Supplementary Information). Obtained results show that *Cm*-Mo_3S_4 forms an intermediate Schottky contact with semiconducting H-MoS_2. The calculated values of

the interface barrier are comparable with the values obtained in the case of T-MoS_2/H-MoS_2 lateral heterostructures (Φ_e^{SM} = 0.70–0.84 eV) [80,82,83]. The strain engineering is considered as one of the promising techniques to change physical and chemical properties in a controllable way [84–86]. The investigation of electronic response on mechanical deformations opens a new field of materials science which is called straintronics [87]. Through controlling the deformation ratio, it is possible to tune the shift of the valence and conduction bands of material and change the electron affinity and ionization potential accordingly. By applying the 4% stretching along the interface (*b* direction in Fig. 3a,d) the value of Mo_3S_4 work function slightly reduced and became equal to 5.03 eV. From another side the values of ionization potential and electron affinity of the MoS_2 phase became equal to 5.87 eV and 4.53 eV respectively. This leads to reduction of the Schottky barrier height (Φ_h^{SM} and Φ_e^{SM}) down to 0.84 eV and 0.50 eV, respectively. In this regard, the controlling deformation can be considered as an effective way of manipulating the Schottky barrier height of the *Cm*-Mo_3S_4/H-MoS_2 heterostructure and whole class of lateral heterostructures.

4. Conclusions

Here we performed the unbiased evolutionary search for 2D structures in the Mo-S system which allowed us to predict a set of phases demonstrating thermodynamic and dynamic stability together with intriguing electronic properties. It is important to note that we considered also metastable phases that were located not higher than 0.1 eV/atom above the convex hull. The newly predicted *Cm*-Mo_3S_4 was found to be metallic according to electronic band structure calculations. *Cm*-Mo_3S_4 could be formed via the application of mechanical deformation of the well-known H-MoS_2 phase with sulfur deficiency (H-Mo_3S_4). The calculated energy profile of the structural transition from defective H-MoS_2 (H-Mo_3S_4) to *Cm*-Mo_3S_4 includes two barriers with the height of the largest one of 1.75 eV per Mo_3S_4 f.u. which can be overcome by temperature exposure.

The proposed way to form a new metallic structure (regions) inside the semiconducting H-MoS_2 by creating the sulfur vacancies with consequent mechanical deformation allows one to avoid the problems of attaching the electrodes to electronic circuits; formed Mo_3S_4 regions may serve as electrodes for MoS_2. For these purposes, we studied the physical and chemical properties of *Cm*-Mo_3S_4/H-MoS_2 lateral heterostructures. It was shown that the conductive properties of the *Cm*-Mo_3S_4 phase are preserved in lateral heterojunction, with the obtained values of Schottky barrier heights Φ_e^{SL} = 0.88 eV and Φ_h^{SL} = 0.84 eV for electrons and holes, respectively. Obtained results show that *Cm*-Mo_3S_4 forms an intermediate Schottky contact with semiconducting H-MoS_2, making it an attractive candidate for use as conductive contact in semiconducting MoS_2-based nanoelectronics device components.

CRediT authorship contribution statement

E.V. Sukhanova: Writing – original draft, Investigation, Conceptualization. **A.G. Kvashnin:** Writing – review & editing. **L.A. Bereznikova:** Investigation. **H.A. Zakaryan:** Investigation, Writing – review & editing. **M.A. Aghamalyan:** Investigation. **D.G. Kvashnin:** Investigation, Writing – review & editing. **Z.I. Popov:** Conceptualization, Writing – review & editing, Supervision, Funding acquisition.

Declaration of Competing Interest

The authors declare that they have no known competing financial interests or personal relationships that could have appeared to influence the work reported in this paper.

Acknowledgements

This work was supported by the Russian Foundation for Basic Research (RFBR) No 20-53-05009 and the Science Committee of the Republic of Armenia SCS 20RF-185 in the frames of the joint research project. The authors are grateful to the Joint Supercomputer Center of the Russian Academy of Sciences and to the Information Technology Centre of Novosibirsk State University for providing access to the cluster computational resources.

Appendix A. Supplementary material

Supplementary data to this article can be found online at https://doi.org/10.1016/j.apsusc.2022.152971.

References

[1] K.S. Novoselov, A.K. Geim, S.V. Morozov, D. Jiang, Y. Zhang, S.V. Dubonos, I. V. Grigorieva, A.A. Firsov, Electric field effect in atomically thin carbon films, Science. 306 (2004) 666–669, https://doi.org/10.1126/science.1102896.
[2] E.S. Kadantsev, P. Hawrylak, Electronic structure of a single MoS_2 monolayer, Solid State Commun. 152 (2012) 909–913, https://doi.org/10.1016/j.ssc.2012.02.005.
[3] X. Wang, X. Guan, X. Ren, T. Liu, W. Huang, J. Cao, C. Jin, Deriving 2D M_2X_3 (M= Mo, W, X= S, Se) by periodic assembly of chalcogen vacancy lines in their MX_2 counterparts, Nanoscale. 12 (15) (2020) 8285–8293, https://doi.org/10.1039/C9NR10144F.
[4] J. Heising, M.G. Kanatzidis, Structure of restacked MoS_2 and WS_2 elucidated by electron crystallography, J. Am. Chem. Soc. 121 (4) (1999) 638–643, https://doi.org/10.1021/ja983043c.
[5] X. Li, S. Meng, J.-T. Sun, Emergence of *d*-orbital magnetic Dirac fermions in a MoS_2 monolayer with squared pentagon structure, Phys. Rev. B. 101 (2020), 144409, https://doi.org/10.1103/PhysRevB.101.144409.
[6] G. Eda, T. Fujita, H. Yamaguchi, D. Voiry, M. Chen, M. Chhowalla, Coherent atomic and electronic heterostructures of single-layer MoS_2, ACS Nano. 6 (8) (2012) 7311–7317, https://doi.org/10.1021/nn302422x.
[7] X. Qian, J. Liu, L. Fu, J.u. Li, Quantum spin Hall effect in two-dimensional transition metal dichalcogenides, Science. 346 (6215) (2014) 1344–1347, https://doi.org/10.1126/science.1256815.
[8] F. Ma, G. Gao, Y. Jiao, Y. Gu, A. Bilic, H. Zhang, Z. Chen, A. Du, Predicting a new phase (T′) of two-dimensional transition metal di-chalcogenides and strain-controlled topological phase transition, Nanoscale. 8 (2016) 4969–4975, https://doi.org/10.1039/C5NR07715J.
[9] Y. Ma, L. Kou, X. Li, Y. Dai, T. Heine, Two-dimensional transition metal dichalcogenides with a hexagonal lattice: Room-temperature quantum spin Hall insulators, Phys. Rev. B. 93 (2016), 035442, https://doi.org/10.1103/PhysRevB.93.035442.
[10] P.-F. Liu, L. Zhou, T. Frauenheim, L.-M. Wu, New quantum spin Hall insulator in two-dimensional MoS_2 with periodically distributed pores, Nanoscale. 8 (2016) 4915–4921, https://doi.org/10.1039/C5NR08842A.
[11] W. Li, M. Guo, G. Zhang, Y.-W. Zhang, Gapless MoS_2 allotrope possessing both massless Dirac and heavy fermions, Phys. Rev. B. 89 (2014), 205402, https://doi.org/10.1103/PhysRevB.89.205402.
[12] S.-M. Nie, Z. Song, H. Weng, Z. Fang, Quantum spin Hall effect in two-dimensional transition-metal dichalcogenide haeckelites, Phys. Rev. B. 91 (2015), 235434, https://doi.org/10.1103/PhysRevB.91.235434.
[13] Y. Sun, C. Felser, B. Yan, Graphene-like Dirac states and quantum spin Hall insulators in square-octagonal MX_2 (M= Mo, W; X= S, Se, Te) isomers, Phys. Rev. B. 92 (2015), 165421, https://doi.org/10.1103/PhysRevB.92.165421.
[14] S. Manzeli, D. Ovchinnikov, D. Pasquier, O.V. Yazyev, A. Kis, 2D transition metal dichalcogenides, Nat. Rev. Mater. 2 (2017) 1–15, https://doi.org/10.1038/natrevmats.2017.33.
[15] O. Samy, S. Zeng, M.D. Birowosuto, A. El Moutaouakil, A Review on MoS_2 Properties, Synthesis, Sensing Applications and Challenges, Crystals. 11 (4) (2021) 355, https://doi.org/10.3390/cryst11040355.
[16] S. Tongay, J. Zhou, C. Ataca, K. Lo, T.S. Matthews, J. Li, J.C. Grossman, J. Wu, Thermally driven crossover from indirect toward direct bandgap in 2D semiconductors: $MoSe_2$ versus MoS_2, Nano Lett. 12 (11) (2012) 5576–5580, https://doi.org/10.1021/nl302584w.
[17] S. Das, H.-Y. Chen, A.V. Penumatcha, J. Appenzeller, High performance multilayer MoS_2 transistors with scandium contacts, Nano Lett. 13 (1) (2013) 100–105, https://doi.org/10.1021/nl303583v.
[18] Z. Xu, J. Lu, X. Zheng, B. Chen, Y. Luo, M.N. Tahir, B. Huang, X. Xia, X. Pan, A critical review on the applications and potential risks of emerging MoS_2 nanomaterials, J. Hazard. Mater. 399 (2020), 123057, https://doi.org/10.1016/j.jhazmat.2020.123057.
[19] J. Theerthagiri, R.A. Senthil, B. Senthilkumar, A.R. Polu, J. Madhavan, M. Ashokkumar, Recent advances in MoS_2 nanostructured materials for energy and environmental applications – A review, J. Solid State Chem. 252 (2017) 43–71, https://doi.org/10.1016/j.jssc.2017.04.041.
[20] Q. Yun, Q. Lu, X. Zhang, C. Tan, H. Zhang, Three-dimensional architectures constructed from transition-metal dichalcogenide nanomaterials for

electrochemical energy storage and conversion, Angew. Chem. Int. Ed. 57 (3) (2018) 626–646, https://doi.org/10.1002/anie.201706426.
[21] Y. Xue, Q. Zhang, W. Wang, H. Cao, Q. Yang, L. Fu, Opening two-dimensional materials for energy conversion and storage: a concept, Adv. Energy Mater. 7 (19) (2017) 1602684, https://doi.org/10.1002/aenm.201602684.
[22] E. Singh, P. Singh, K.S. Kim, G.Y. Yeom, H.S. Nalwa, Flexible Molybdenum Disulfide (MoS_2) Atomic Layers for Wearable Electronics and Optoelectronics, ACS Appl. Mater. Interfaces. 11 (2019) 11061–11105, https://doi.org/10.1021/acsami.8b19859.
[23] D. Lembke, S. Bertolazzi, A. Kis, Single-layer MoS_2 electronics, Acc. Chem. Res. 48 (1) (2015) 100–110, https://doi.org/10.1021/ar500274q.
[24] M. Donarelli, L. Ottaviano, 2D materials for gas sensing applications: a review on graphene oxide, MoS_2, WS_2 and phosphorene, Sensors. 18 (2018) 3638, https://doi.org/10.3390/s18113638.
[25] E.V. Sukhanova, D.G. Kvashnin, Z.I. Popov, Induced spin polarization in graphene via interactions with halogen doped MoS_2 and $MoSe_2$ monolayers by DFT calculations, Nanoscale. 12 (2020) 23248–23258, https://doi.org/10.1039/D0NR06287A.
[26] Z. Liang, R. Shen, Y.H. Ng, P. Zhang, Q. Xiang, X. Li, A review on 2D MoS_2 cocatalysts in photocatalytic H_2 production, J. Mater. Sci. Technol. 56 (2020) 89–121, https://doi.org/10.1016/j.jmst.2020.04.032.
[27] Y. Yoon, K. Ganapathi, S. Salahuddin, How good can monolayer MoS_2 transistors be? Nano Lett. 11 (9) (2011) 3768–3773, https://doi.org/10.1021/nl2018178.
[28] B. Radisavljevic, A. Radenovic, J. Brivio, V. Giacometti, A. Kis, Single-layer MoS_2 transistors, Nat. Nanotechnol. 6 (3) (2011) 147–150, https://doi.org/10.1038/nnano.2010.279.
[29] Y. Pan, J. Gu, H. Tang, X. Zhang, J. Li, B. Shi, J. Yang, H. Zhang, J. Yan, S. Liu, H. Hu, M. Wu, J. Lu, Reexamination of the Schottky barrier heights in monolayer MoS_2 field-effect transistors, ACS Appl. Nano Mater. 2 (8) (2019) 4717–4726, https://doi.org/10.1021/acsanm.9b00200.
[30] J.-R. Chen, P.M. Odenthal, A.G. Swartz, G.C. Floyd, H. Wen, K.Y. Luo, R. K. Kawakami, Control of Schottky barriers in single layer MoS_2 transistors with ferromagnetic contacts, Nano Lett. 13 (7) (2013) 3106–3110, https://doi.org/10.1021/nl4010157.
[31] S.-S. Chee, D. Seo, H. Kim, H. Jang, S. Lee, S.P. Moon, K.H. Lee, S.W. Kim, H. Choi, M.-H. Ham, Lowering the Schottky barrier height by graphene/Ag electrodes for high-mobility MoS_2 field-effect transistors, Adv. Mater. 31 (2019) 1804422, https://doi.org/10.1002/adma.201804422.
[32] H. Yuan, G. Cheng, L. You, H. Li, H. Zhu, W. Li, J.J. Kopanski, Y.S. Obeng, A. R. Hight Walker, D.J. Gundlach, C.A. Richter, D.E. Ioannou, Q. Li, Influence of metal–MoS_2 interface on MoS_2 transistor performance: Comparison of Ag and Ti contacts, ACS Appl. Mater. Interfaces. 7 (2) (2015) 1180–1187, https://doi.org/10.1021/am506921y.
[33] H. Fang, M. Tosun, G. Seol, T.C. Chang, K. Takei, J. Guo, A. Javey, Degenerate n-doping of few-layer transition metal dichalcogenides by potassium, Nano Lett. 13 (5) (2013) 1991–1995, https://doi.org/10.1021/nl400044m.
[34] Y. Du, H. Liu, A.T. Neal, M. Si, P.D. Ye, Molecular Doping of Multilayer MoS_2 Field-Effect Transistors: Reduction in Sheet and Contact Resistances, IEEE Electron Device Lett. 34 (10) (2013) 1328–1330, https://doi.org/10.1109/LED.2013.2277311.
[35] Y. Kim, A.R. Kim, J.H. Yang, K.E. Chang, J.-D. Kwon, S.Y. Choi, J. Park, K.E. Lee, D.-H. Kim, S.M. Choi, K.H. Lee, B.H. Lee, M.G. Hahm, B. Cho, Alloyed 2D Metal-Semiconductor Heterojunctions: Origin of Interface States Reduction and Schottky Barrier Lowering, Nano Lett. 16 (2016) 5928–5933, https://doi.org/10.1021/acs.nanolett.6b02893.
[36] R. Kappera, D. Voiry, S.E. Yalcin, W. Jen, M. Acerce, S. Torrel, B. Branch, S. Lei, W. Chen, S. Najmaei, J. Lou, P.M. Ajayan, G. Gupta, A.D. Mohite, M. Chhowalla, Metallic 1T phase source/drain electrodes for field effect transistors from chemical vapor deposited MoS_2, APL Mater 2 (2014) 092516, https://doi.org/10.1063/1.4896077.
[37] S. Cho, S. Kim, J.H. Kim, J. Zhao, J. Seok, D.H. Keum, J. Baik, D.-H. Choe, K. J. Chang, K. Suenaga, S.W. Kim, Y.H. Lee, H. Yang, Phase patterning for ohmic homojunction contact in $MoTe_2$, Science. 349 (2015) 625–628, https://doi.org/10.1126/science.aab3175.
[38] H.-J. Chuang, B. Chamlagain, M. Koehler, M.M. Perera, J. Yan, D. Mandrus, D. Tománek, Z. Zhou, Low-Resistance 2D/2D Ohmic Contacts: A Universal Approach to High-Performance WSe_2, MoS_2, and $MoSe_2$ Transistors, Nano Lett. 16 (2016) 1896–1902, https://doi.org/10.1021/acs.nanolett.5b05066.
[39] D.G. Kvashnin, L.A. Chernozatonskii, Electronic and transport properties of heterophase compounds based on MoS_2, JETP Lett. 105 (4) (2017) 250–254, https://doi.org/10.1134/S0021364017040117.
[40] E.C. Hadland, F. Göhler, G. Mitchson, S.S. Fender, C. Schmidt, D.R.T. Zahn, T. Seyller, D.C. Johnson, Synthesis and Properties of $(BiSe)_{0.97}MoSe_2$: A Heterostructure Containing Both 2H-$MoSe_2$ and 1T-$MoSe_2$, Chem. Mater. 31 (15) (2019) 5824–5831, https://doi.org/10.1021/acs.chemmater.9b01899.
[41] X. Duan, C. Wang, J.C. Shaw, R. Cheng, Y.u. Chen, H. Li, X. Wu, Y. Tang, Q. Zhang, A. Pan, J. Jiang, R. Yu, Y.u. Huang, X. Duan, Lateral epitaxial growth of two-dimensional layered semiconductor heterojunctions, Nat. Nanotechnol. 9 (12) (2014) 1024–1030, https://doi.org/10.1038/nnano.2014.222.
[42] Y. Gong, J. Lin, X. Wang, G. Shi, S. Lei, Z. Lin, X. Zou, G. Ye, R. Vajtai, B. I. Yakobson, H. Terrones, M. Terrones, B. Tay, J. Lou, S.T. Pantelides, Z. Liu, W. u. Zhou, P.M. Ajayan, Vertical and in-plane heterostructures from WS_2/MoS_2 monolayers, Nat. Mater. 13 (12) (2014) 1135–1142, https://doi.org/10.1038/nmat4091.
[43] P.K. Sahoo, S. Memaran, Y. Xin, L. Balicas, H.R. Gutiérrez, One-pot growth of two-dimensional lateral heterostructures via sequential edge-epitaxy, Nature. 553 (7686) (2018) 63–67, https://doi.org/10.1038/nature25155.
[44] S. Kretschmer, H.-P. Komsa, P. Bøggild, A.V. Krasheninnikov, Structural Transformations in Two-Dimensional Transition-Metal Dichalcogenide MoS_2 under an Electron Beam: Insights from First-Principles Calculations, J. Phys. Chem. Lett. 8 (2017) 3061–3067, https://doi.org/10.1021/acs.jpclett.7b01177.
[45] Y.-C. Lin, D.O. Dumcenco, Y.-S. Huang, K. Suenaga, Atomic mechanism of the semiconducting-to-metallic phase transition in single-layered MoS_2, Nat. Nanotechnol. 9 (2014) 391–396, https://doi.org/10.1038/nnano.2014.64.
[46] G. Gao, Y. Jiao, F. Ma, Y. Jiao, E. Waclawik, A. Du, Charge mediated semiconducting-to-metallic phase transition in molybdenum disulfide monolayer and hydrogen evolution reaction in new 1T′ phase, J. Phys. Chem. C. 119 (23) (2015) 13124–13128, https://doi.org/10.1021/acs.jpcc.5b04658.
[47] G. Eda, H. Yamaguchi, D. Voiry, T. Fujita, M. Chen, M. Chhowalla, Photoluminescence from chemically exfoliated MoS_2, Nano Lett. 11 (12) (2011) 5111–5116, https://doi.org/10.1021/nl201874w.
[48] A.I. Boldyrev, L.-S. Wang, Beyond classical stoichiometry: experiment and theory, J. Phys. Chem. A. 105 (2001) 10759–10775, https://doi.org/10.1021/jp0122629.
[49] Y. Chen, J.-J. Deng, W.-W. Yao, J.I. Gurti, W. Li, W.-J. Wang, J.-X. Yao, X.-L. Ding, Non-stoichiometric molybdenum sulfide clusters and their reactions with the hydrogen molecule, Phys. Chem. Chem. Phys. 23 (1) (2021) 347–355, https://doi.org/10.1039/d0cp04457a.
[50] T. Joseph, M. Ghorbani-Asl, A.G. Kvashnin, K.V. Larionov, Z.I. Popov, P.B. Sorokin, A.V. Krasheninnikov, Nonstoichiometric phases of two-dimensional transition-metal dichalcogenides: from chalcogen vacancies to pure metal membranes, J. Phys. Chem. Lett. 10 (2019) 6492–6498, https://doi.org/10.1021/acs.jpclett.9b02529.
[51] A.R. Oganov, C.W. Glass, Crystal structure prediction using ab initio evolutionary techniques: Principles and applications, J. Chem. Phys. 124 (2006), 244704, https://doi.org/10.1063/1.2210932.
[52] A.O. Lyakhov, A.R. Oganov, H.T. Stokes, Q. Zhu, New developments in evolutionary structure prediction algorithm USPEX, Comput. Phys. Commun. 184 (4) (2013) 1172–1182, https://doi.org/10.1016/j.cpc.2012.12.009.
[53] A.R. Oganov, A.O. Lyakhov, M. Valle, How Evolutionary Crystal Structure Prediction Works and Why, Acc. Chem. Res. 44 (2011) 227–237, https://doi.org/10.1021/ar1001318.
[54] A.O. Lyakhov, A.R. Oganov, H.T. Stokes, Q. Zhu, New developments in evolutionary structure prediction algorithm USPEX, Comput. Phys. Commun. 184 (2013) 1172–1182, https://doi.org/10.1016/j.cpc.2012.12.009.
[55] G. Kresse, J. Furthmüller, Efficient iterative schemes for *ab initio* total-energy calculations using a plane-wave basis set, Phys. Rev. B. 54 (16) (1996) 11169–11186, https://doi.org/10.1103/PhysRevB.54.11169.
[56] G. Kresse, J. Furthmüller, Efficiency of ab-initio total energy calculations for metals and semiconductors using a plane-wave basis set, Comput. Mater. Sci. 6 (1996) 15–50, https://doi.org/10.1016/0927-0256(96)00008-0.
[57] G. Kresse, J. Hafner, Ab initio molecular-dynamics simulation of the liquid-metal-amorphous-semiconductor transition in germanium, Phys. Rev. B. 49 (1994) 14251–14269, https://doi.org/10.1103/PhysRevB.49.14251.
[58] J.P. Perdew, K. Burke, M. Ernzerhof, Generalized Gradient Approximation Made Simple, Phys. Rev. Lett. 77 (1996) 3865–3868, https://doi.org/10.1103/PhysRevLett.77.3865.
[59] P.E. Blöchl, Projector augmented-wave method, Phys. Rev. B. 50 (1994) 17953–17979, https://doi.org/10.1103/PhysRevB.50.17953.
[60] H.J. Monkhorst, J.D. Pack, Special points for Brillouin-zone integrations, Phys Rev B. 13 (1976) 5188–5192, https://doi.org/10.1103/PhysRevB.13.5188.
[61] A. Togo, I. Tanaka, First principles phonon calculations in materials science, Scr. Mater. 108 (2015) 1–5, https://doi.org/10.1016/j.scriptamat.2015.07.021.
[62] R.A. Olsen, G.J. Kroes, G. Henkelman, A. Arnaldsson, H. Jónsson, Comparison of methods for finding saddle points without knowledge of the final states, J. Chem. Phys. 121 (20) (2004) 9776–9792, https://doi.org/10.1063/1.1809574.
[63] G. Henkelman, H. Jónsson, Improved tangent estimate in the nudged elastic band method for finding minimum energy paths and saddle points, J. Chem. Phys. 113 (22) (2000) 9978–9985, https://doi.org/10.1063/1.1323224.
[64] K. Momma, F. Izumi, VESTA 3 for three-dimensional visualization of crystal, volumetric and morphology data, J. Appl. Crystallogr. 44 (2011) 1272–1276, https://doi.org/10.1107/S0021889811038970.
[65] Q. Liu, X. Li, Q. He, A. Khalil, D. Liu, T. Xiang, X. Wu, L. Song, Gram-scale aqueous synthesis of stable few-layered 1T-MoS_2: applications for visible-light-driven photocatalytic hydrogen evolution, Small. 11 (2015) 5556–5564, https://doi.org/10.1002/smll.201501822.
[66] H. Xu, D. Han, Y. Bao, F. Cheng, Z. Ding, S.J.R. Tan, K.P. Loh, Observation of Gap Opening in 1T′ Phase MoS_2 Nanocrystals, Nano Lett. 18 (2018) 5085–5090, https://doi.org/10.1021/acs.nanolett.8b01953.
[67] J. Sun, X. Li, W. Guo, M. Zhao, X. Fan, Y. Dong, C. Xu, J. Deng, Y. Fu, Synthesis methods of two-dimensional MoS_2: A brief review, Crystals. 7 (2017) 198, https://doi.org/10.3390/cryst7070198.
[68] D.-M. Tang, D.G. Kvashnin, S. Najmaei, Y. Bando, K. Kimoto, P. Koskinen, P. M. Ajayan, B.I. Yakobson, P.B. Sorokin, J. Lou, Nanomechanical cleavage of molybdenum disulphide atomic layers, Nat. Commun. 5 (2014) 1–8, https://doi.org/10.1038/ncomms4631.
[69] Y.D. Kuang, L. Lindsay, S.Q. Shi, G.P. Zheng, Tensile strains give rise to strong size effects for thermal conductivities of silicene, germanene and stanene, Nanoscale. 8 (2016) 3760–3767, https://doi.org/10.1039/C5NR08231E.

[70] A.S. Nissimagoudar, A. Manjanath, A.K. Singh, Diffusive nature of thermal transport in stanene, Phys. Chem. Chem. Phys. 18 (2016) 14257–14263, https://doi.org/10.1039/C5CP07957H.
[71] L. Zha, J. Tian, J. Lu, Y. Zhang, X. Wei, J. Cao, Electronic properties of the one-dimensional interfaces in two dimensional lateral $(MoS_2)_m/(Mo_2S_3)_m$ heterostructures, Chem. Phys. Lett. 778 (2021), 138761, https://doi.org/10.1016/j.cplett.2021.138761.
[72] G.A. Henkelman, A. Arnaldsson, H. Jónsson, A fast and robust algorithm for Bader decomposition of charge density, Comput. Mater. Sci. 36 (2006) 354–360, https://doi.org/10.1016/j.commatsci.2005.04.010.
[73] F. Mouhat, F.-X. Coudert, Necessary and sufficient elastic stability conditions in various crystal systems, Phys. Rev. B. 90 (2014), 224104, https://doi.org/10.1103/PhysRevB.90.224104.
[74] H.-P. Komsa, A.V. Krasheninnikov, Engineering the Electronic Properties of Two-Dimensional Transition Metal Dichalcogenides by Introducing Mirror Twin Boundaries, Adv. Electron. Mater. 3 (2017) 1600468, https://doi.org/10.1002/aelm.201600468.
[75] M. Ghorbani-Asl, S. Kretschmer, D.E. Spearot, A.V. Krasheninnikov, Two-dimensional MoS_2 under ion irradiation: from controlled defect production to electronic structure engineering, 2D Mater 4 (2017) 025078, https://doi.org/10.1088/2053-1583/aa6b17.
[76] J. Xia, J. Wang, D. Chao, Z. Chen, Z. Liu, J.-L. Kuo, J. Yan, Z.X. Shen, Phase evolution of lithium intercalation dynamics in 2H-MoS_2, Nanoscale. 9 (2017) 7533–7540, https://doi.org/10.1039/C7NR02028G.
[77] D. Nasr Esfahani, O. Leenaerts, H. Sahin, B. Partoens, F.M. Peeters, Structural Transitions in Monolayer MoS_2 by Lithium Adsorption, J. Phys. Chem. C. 119 (2015) 10602–10609, https://doi.org/10.1021/jp510083w.
[78] A.M. van der Zande, P.Y. Huang, D.A. Chenet, T.C. Berkelbach, Y. You, G.-H. Lee, T.F. Heinz, D.R. Reichman, D.A. Muller, J.C. Hone, Grains and grain boundaries in highly crystalline monolayer molybdenum disulphide, Nat. Mater. 12 (2013) 554–561, https://doi.org/10.1038/nmat3633.
[79] H. Kim, H.J. Choi, Thickness dependence of work function, ionization energy, and electron affinity of Mo and W dichalcogenides from DFT and GW calculations, Phys. Rev. B. 103 (2021), 085404, https://doi.org/10.1103/PhysRevB.103.085404.
[80] M. Houssa, K. Iordanidou, A. Dabral, A. Lu, G. Pourtois, V. Afanasiev, A. Stesmans, Contact resistance at MoS_2-based 2D metal/semiconductor lateral heterojunctions, ACS Appl. Nano Mater. 2 (2) (2019) 760–766, https://doi.org/10.1021/acsanm.8b01963.
[81] M. Houssa, K. Iordanidou, A. Dabral, A. Lu, R. Meng, G. Pourtois, V.V. Afanas'ev, A. Stesmans, Contact resistance at graphene/MoS_2 lateral heterostructures, Appl. Phys. Lett. 114 (2019) 163101, https://doi.org/10.1063/1.5083133.
[82] Z.-Q. Fan, X.-W. Jiang, J.-W. Luo, L.-Y. Jiao, R. Huang, S.-S. Li, L.-W. Wang, In-plane Schottky-barrier field-effect transistors based on 1T/2H heterojunctions of transition-metal dichalcogenides, Phys. Rev. B. 96 (2017), 165402, https://doi.org/10.1103/PhysRevB.96.165402.
[83] Y. Katagiri, T. Nakamura, A. Ishii, C. Ohata, M. Hasegawa, S. Katsumoto, T. Cusati, A. Fortunelli, G. Iannaccone, G. Fiori, S. Roche, J. Haruyama, Gate-Tunable Atomically Thin Lateral MoS_2 Schottky Junction Patterned by Electron Beam, Nano Lett. 16 (2016) 3788–3794, https://doi.org/10.1021/acs.nanolett.6b01186.
[84] J. Qi, Y.-W. Lan, A.Z. Stieg, J.-H. Chen, Y.-L. Zhong, L.-J. Li, C.-D. Chen, Y. Zhang, K.L. Wang, Piezoelectric effect in chemical vapour deposition-grown atomic-monolayer triangular molybdenum disulfide piezotronics, Nat. Commun. 6 (2015) 7430, https://doi.org/10.1038/ncomms8430.
[85] Z. Zhang, L. Li, J. Horng, N.Z. Wang, F. Yang, Y. Yu, Y. Zhang, G. Chen, K. Watanabe, T. Taniguchi, X.H. Chen, F. Wang, Y. Zhang, Strain-Modulated Bandgap and Piezo-Resistive Effect in Black Phosphorus Field-Effect Transistors, Nano Lett. 17 (2017) 6097–6103, https://doi.org/10.1021/acs.nanolett.7b02624.
[86] F. Guo, Y. Lyu, M.B. Jedrzejczyk, Y. Zhao, W.F. Io, G. Bai, W. Wu, J. Hao, Piezoelectric biaxial strain effects on the optical and photoluminescence spectra of 2D III–VI compound α-In_2Se_3 nanosheets, Appl. Phys. Lett. 116 (2020), 113101, https://doi.org/10.1063/5.0001795.
[87] A.A. Bukharaev, A.K. Zvezdin, A.P. Pyatakov, Y.K. Fetisov, Straintronics: a new trend in micro- and nanoelectronics and materials science, Phys.-Uspekhi. 61 (12) (2018) 1175–1212, https://doi.org/10.3367/UFNe.2018.01.038279.